Supporting information for:

Comparing serial X-ray crystallography and microcrystal electron diffraction (MicroED) as methods for routine structure determination from small macromolecular crystals

Alexander M Wolff[1,2], Iris D Young[2,3], Raymond G Sierra[4], Aaron S Brewster[3], Michael W Martynowycz[5,6] Eriko Nango[7,8], Michihiro Sugahara[7], Takanori Nakane[9,†], Kazutaka Ito[2,10], Andrew Aquila[4], Asmit Bhowmik[3], Justin T Biel[1,2], Sergio Carbajo[4], Aina E Cohen[11]; Saul Cortez[12], Ana Gonzalez[11], Tomoya Hino[13,14], Dohyun Im[8], Jake D Koralek[4], Minoru Kubo[7,15], Tomas S Lazarou[16], Takashi Nomura[7], Shigeki Owada[7,22], Avi Samelson[17], Tomoyuki Tanaka[7,8], Rie Tanaka[7,8], Erin M Thompson[2,18], Henry van den Bedem[19], Rahel A Woldeyes[2,18], Fumiaki Yumoto[20], Wei Zhao[21], Kensuke Tono[7,22], Sébastien Boutet[4], So Iwata[7,8], Tamir Gonen[5,6,23], Nicholas K Sauter[3], James S Fraser[2], Michael C Thompson[2,#]

1. *Graduate Program in Biophysics, University of California, San Francisco, San Francisco, CA, USA*
2. *Department of Bioengineering and Therapeutic Sciences, University of California, San Francisco, San Francisco, CA, USA*
3. *Molecular Biophysics and Integrated Bioimaging Division, Lawrence Berkeley National Laboratory, Berkeley, CA, USA*
4. *Linac Coherent Light Source, SLAC National Accelerator Laboratory, Menlo Park, CA, USA*
5. *Howard Hughes Medical Institute, University of California, Los Angeles, Los Angeles, CA, USA*
6. *Department of Biological Chemistry, University of California, Los Angeles, Los Angeles, CA, USA*
7. *RIKEN SPring-8 Center, 1-1-1 Kouto, Sayo-cho, Sayo-gun, Hyogo, 679-5148, Japan*
8. *Department of Cell Biology, Graduate School of Medicine, Kyoto University, Yoshidakonoe-cho, Sakyo-ku, Kyoto 606-8501, Japan*
9. *Department of Biological Science, Graduate School of Science, The University of Tokyo, Tokyo, Japan*
10. *Laboratory for Drug Discovery, Pharmaceuticals Research Center, Asahi Kasei Pharma Corporation, 632-1 Mifuku, Izunokuni-shi, Shizuoka 410-2321, Japan.*
11. *SSRL, SLAC National Accelerator Laboratory, Menlo Park, CA, USA*
12. *Department of Biology, San Francisco State University, San Francisco, CA, USA*
13. *Department of Chemistry and Biotechnology, Graduate School of Engineering, Tottori University, 4-101, Koyama-cho Minami, Tottori 680-8552, Japan*
14. *Center for Research on Green Sustainable Chemistry, Tottori University, Tottori, Japan*
15. *Graduate School of Life Science, University of Hyogo, Ako-gun, Hyogo 678-1297, Japan*
16. *Department of Chemistry, New York University, New York, NY, USA*
17. *Institute for Neurodegenerative Diseases, University of California, San Francisco, San Francisco, CA, USA*
18. *Graduate Program in Chemistry and Chemical Biology, University of California, San Francisco, San Francisco, CA, USA*
19. *Bioscience Department, SLAC National Accelerator Laboratory, Menlo Park, CA, USA*
20. *Structural Biology Research Center, Institute of Materials Structure Science, KEK/High Energy Accelerator Research Organization, Tsukuba, Ibaraki 305-0034, Japan*
21. *Department of Biology and Biological Engineering, California Institute of Technology, Pasadena, CA, USA*
22. *Japan Synchrotron Radiation Research Institute, 1-1-1 Kouto, Sayo, Hyogo 679-5198, Japan*
23. *Department of Physiology, University of California, Los Angeles, Los Angeles, CA*

†Present address: MRC laboratory of molecular biology, Cambridge, UK

 # - correspondence: mct.ucsf@gmail.com

Table of Contents:

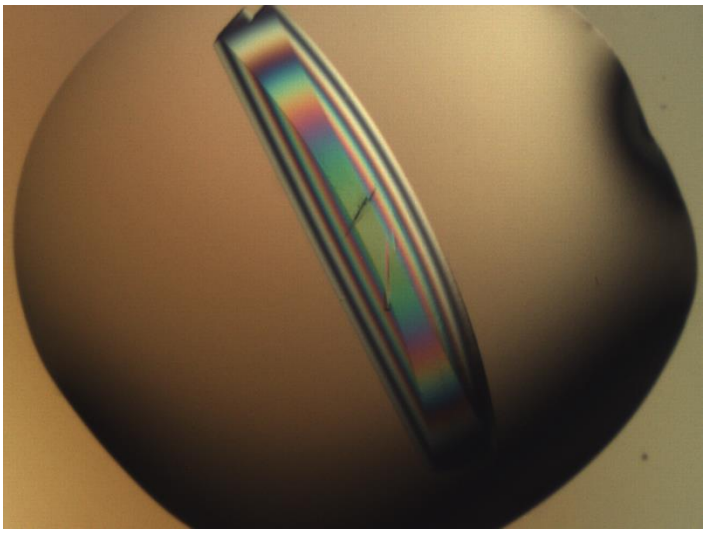

Supporting Figure 1. Previously, CypA crystallization conditions were optimized to produce very large single crystals. The pictured crystal (viewed using a cross-polarizer) was over 1 mm long and was visible to the naked eye.

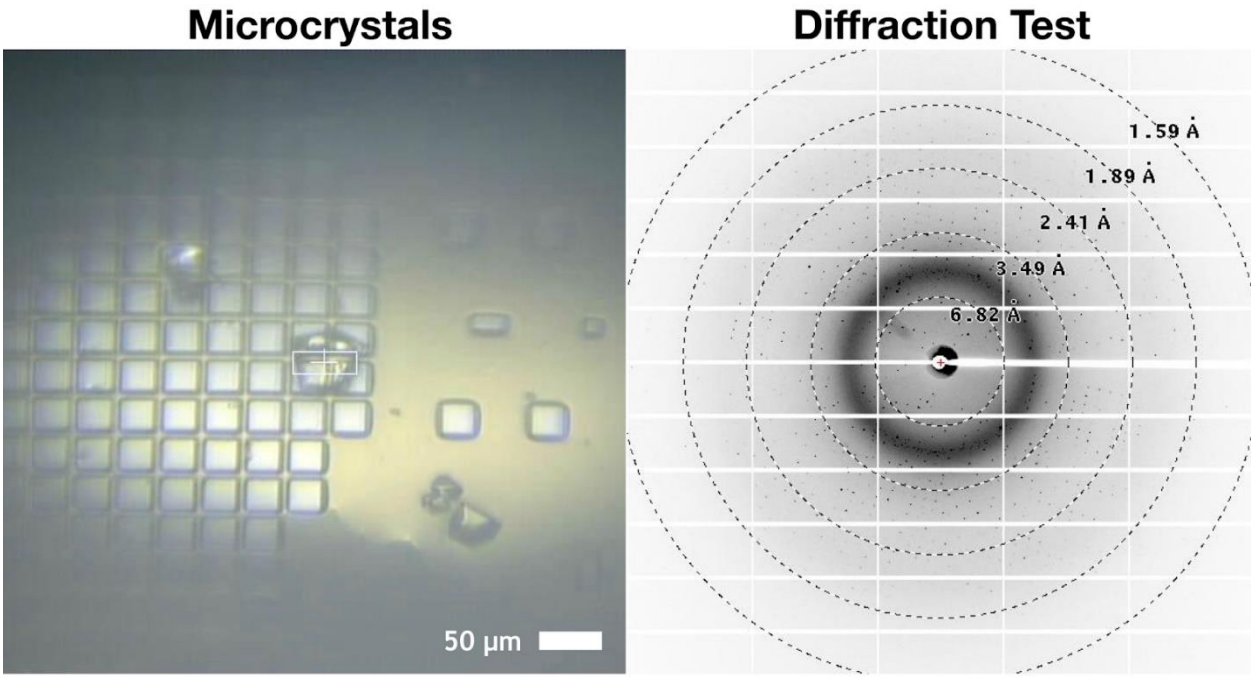

Supporting Figure 2. Image of microcrystals on a Mitegen micromesh grid (left) and the subsequent diffraction from one of these crystals (right). Crystals were 20-50 µm in size, and diffracted to the edge of the detector at 1.59 Å.

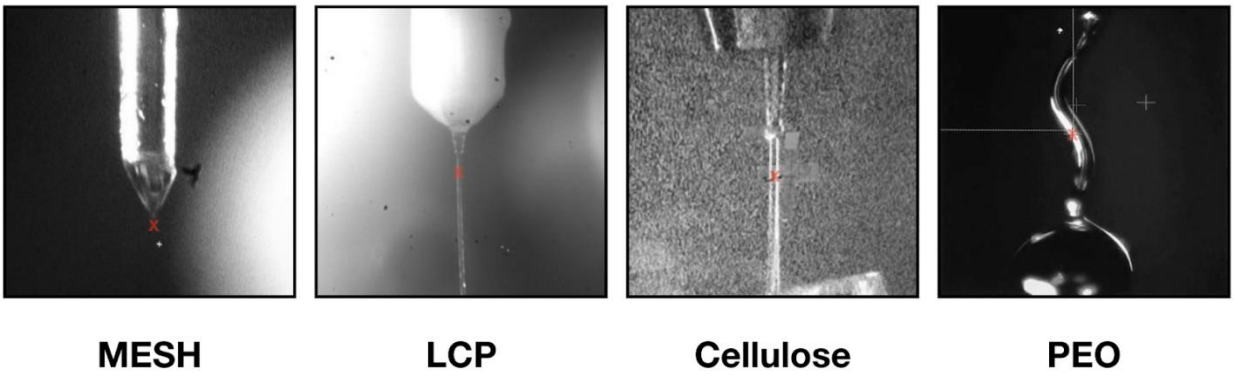

Supporting Figure 3. Images of jets delivering microcrystal slurries to the XFEL interaction point (red "x" in each image). Minimal viscogens were added to the crystalline slurry for the MESH injector system. When using a viscous extrusion type of injector, a variety of carrier media were tested, including LCP, Cellulose, and PEO.

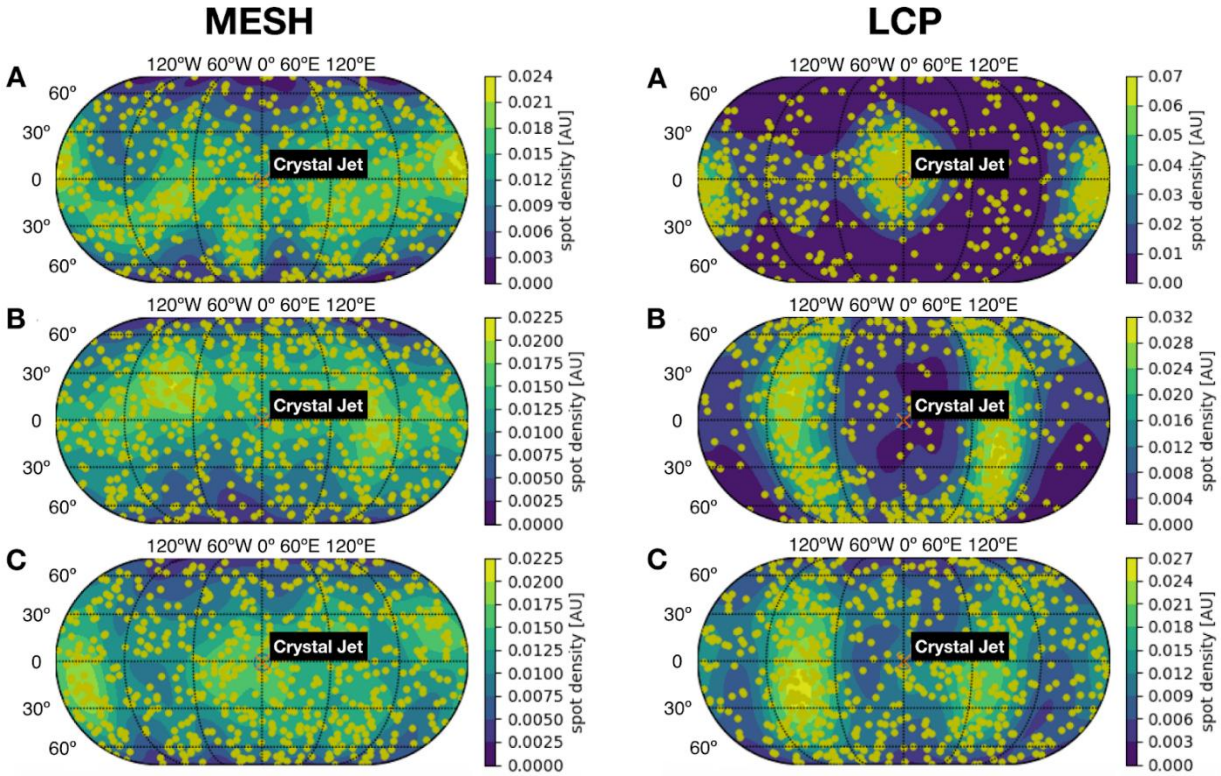

Supporting Figure 4. Map of crystal orientations from the MESH data collection (left panel) and from the LCP data collection (right panel). A subset of each dataset is shown for visual clarity. The orientations appear evenly distributed for the MESH data, with no major bias introduced by the electric field created by the injection system. The viscosity of the LCP carrier media appears to have induced an orientation bias, but did not prohibit collection of a complete dataset with high redundancy.

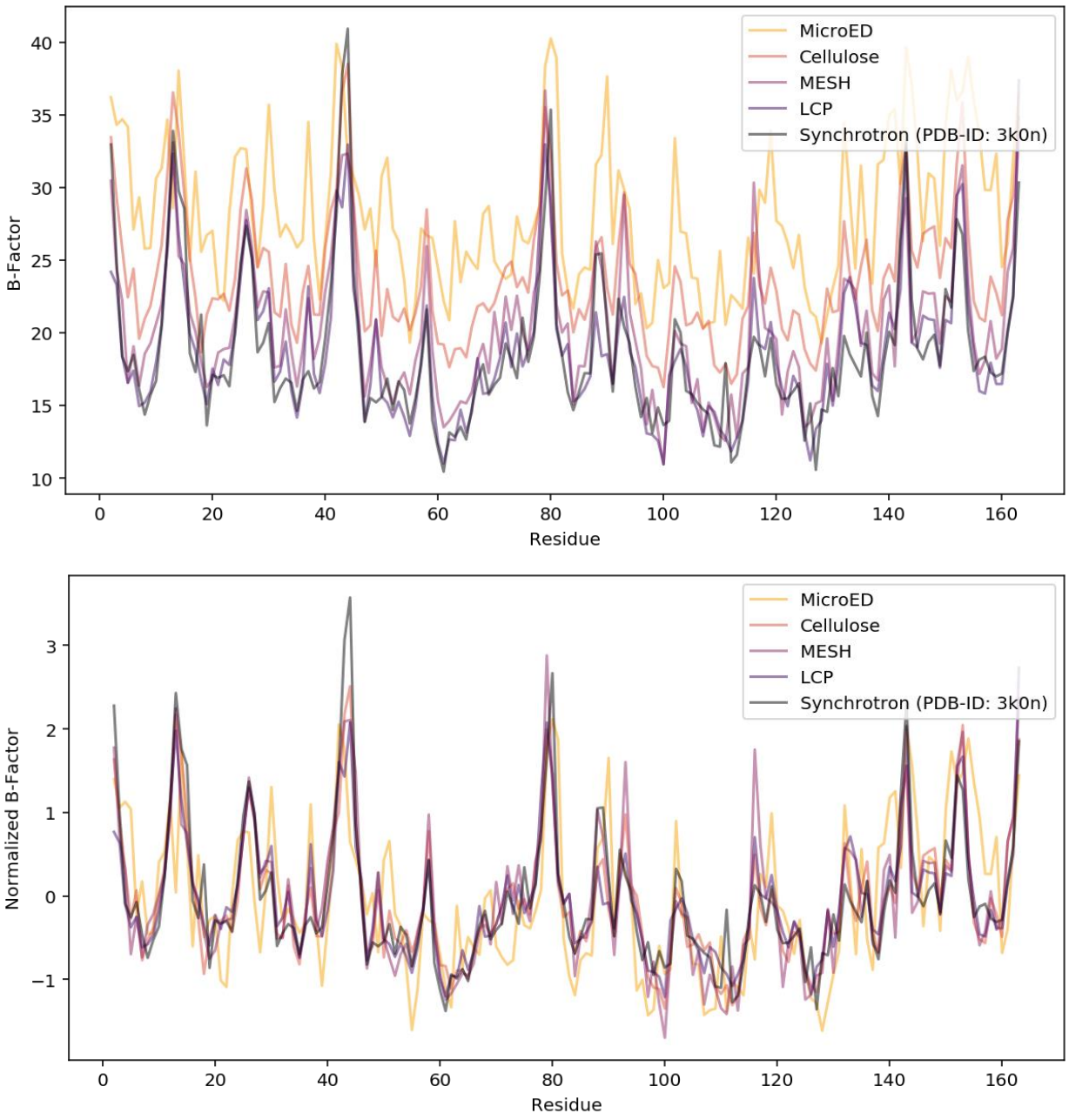

Supporting Figure 5. Raw (top) and normalized (bottom) B-factor per residue across data sets. A previously published structure, solved at room temperature using rotational collection from a single crystal (PDB ID *3K0N*) is provided for reference. Most variation is systematic, and thus is removed by normalization.

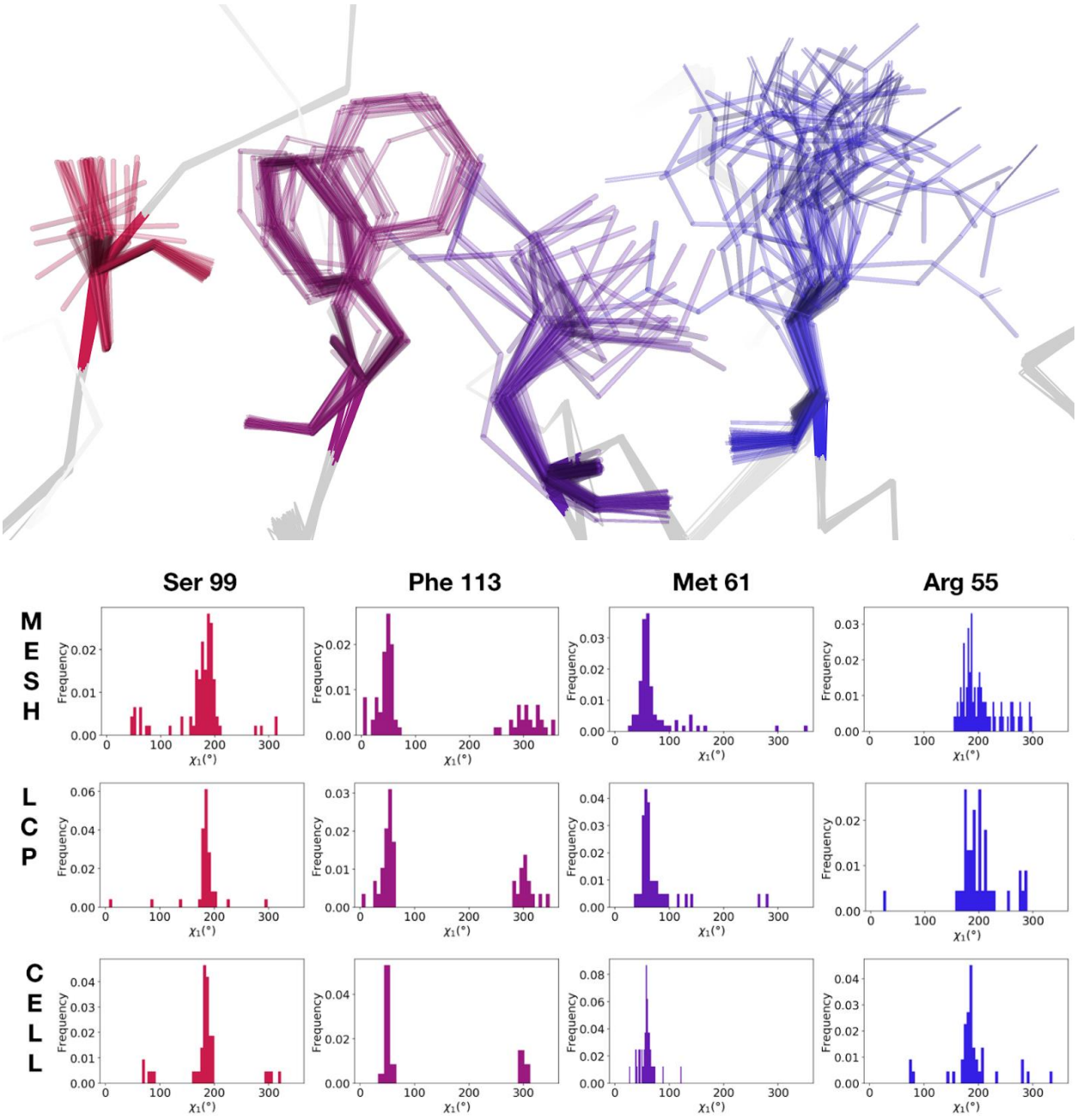

Supporting Figure 6. Visualization of the ensemble of conformers generated via phenix.ensemble_refine for the three serial XFEL datasets. The analysis focuses on a network of amino acid side chains that are known to be dynamic and important for function. In the top panel, the ensemble model for the cellulose dataset is displayed. Sticks are shown for the residues of interest (R55, M61, S99, F113), while the backbone is displayed as a ribbon for the rest of the structure. In the bottom panel, histograms of the distribution of chi1 angles are plotted for each of the four residues from the respective ensemble. The comparison shows that ensembles derived from the different serial X-ray experiments are essentially equivalent.

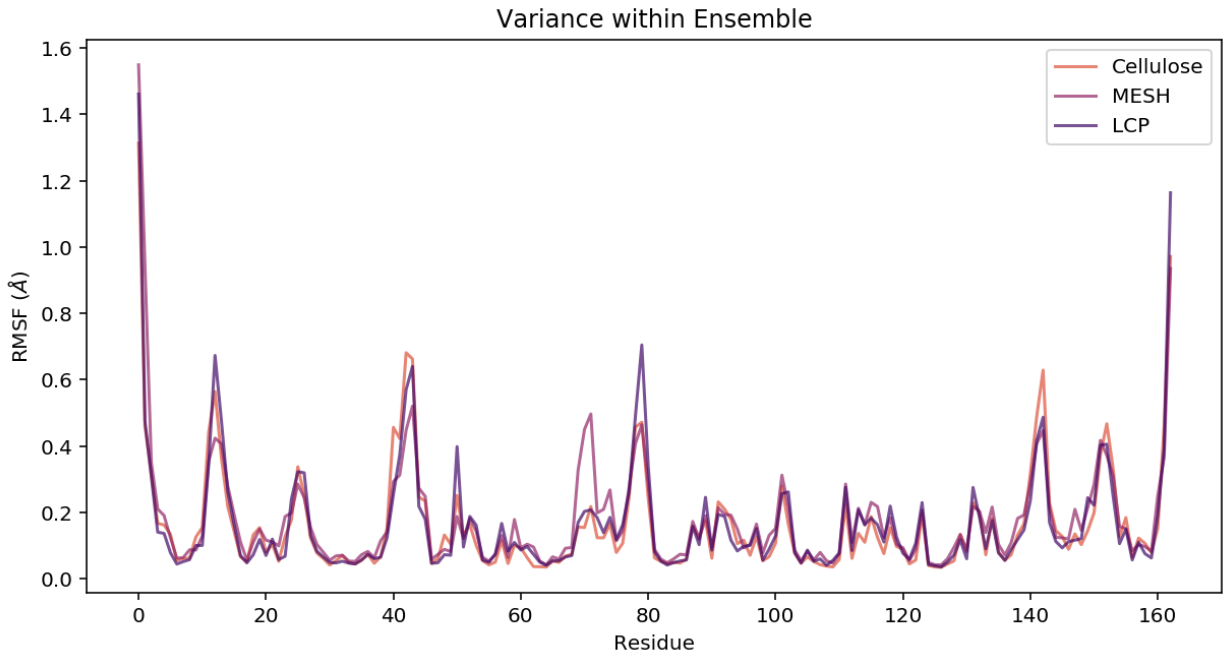

Supporting Figure 7. Average RMSF per residue for each ensemble generated for the serial XFEL datasets. A loop containing residues 64-74 samples more conformations in the MESH ensemble than in the other two.

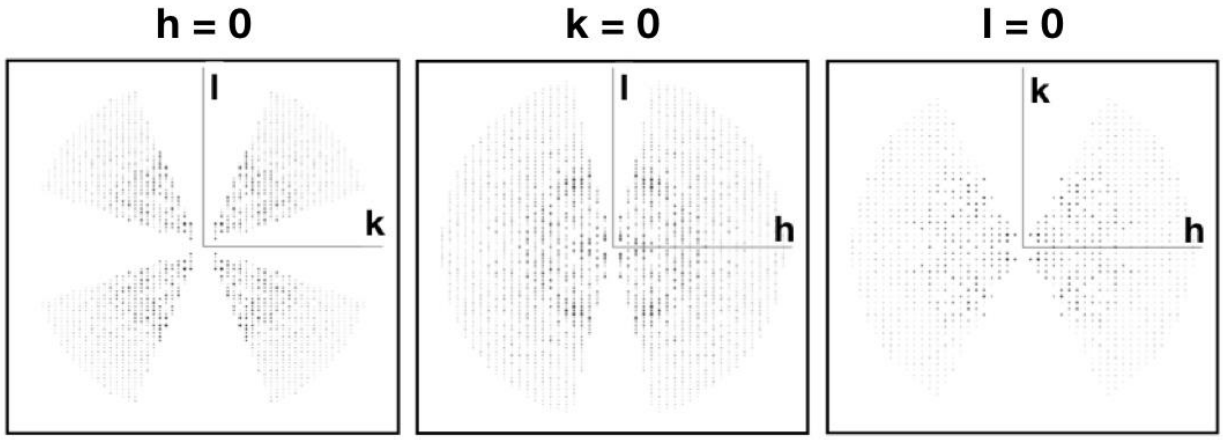

Supporting Figure 8. MicroED data visualized on two-dimensional slices of the reciprocal lattice. Measured reflections are visualized in black. Missing measurements along the kl plane may contribute to challenges in assignment of unit cell dimensions.

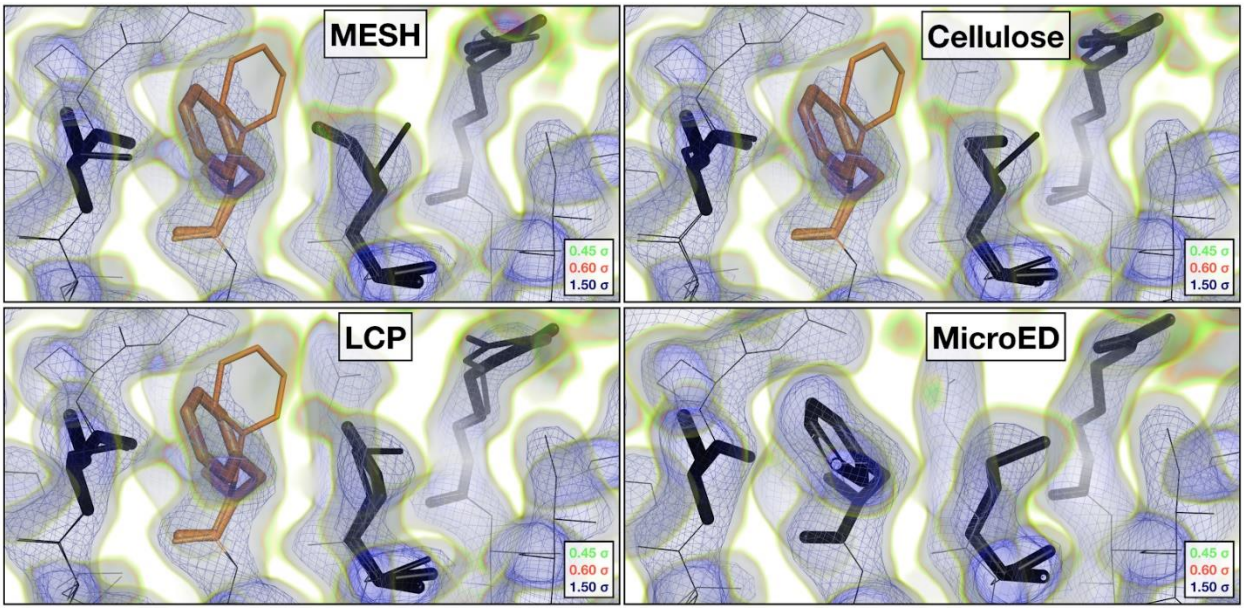

Supporting Figure 9. Visualization of all four datasets truncated at 2.5 Å. Comparison of the 2mFoFc maps and refined multi-conformer models reveals evidence for alternative conformations in the room temperature data (MESH, LCP, Cellulose), while cryogenic data (MicroED) supports a single conformer model.